Spatial conversion profiles within an SCR in a test exhaust system with injection of ammonia gas modelled in CFD using the porous medium approach

Sturgess, M.P. , Benjamin, S.F. and Roberts, C.A.

SAE International™

Spatial Conversion Profiles within an SCR in a Test Exhaust System with Injection of Ammonia Gas Modelled in CFD using the Porous Medium Approach

2010-01-2089
Published
10/25/2010

M. P. Sturgess, S. F. Benjamin and C. A. Roberts
Coventry University

ABSTRACT

Modelling of SCR in diesel exhaust systems with injection of urea spray is complex and challenging but many models use only the conversion observed at the brick exit as a test of the model. In this study, the case modelled is simplified by injecting ammonia gas in nitrogen in place of urea, but the spatial conversion profiles along the SCR brick length at steady state are investigated. This is a more rigorous way of assessing the ability of the model to simulate observations made on a test exhaust system. The data have been collected by repeated engine tests on eight different brick lengths, all which were shorter than a standard sized SCR. The tests have been carried out for supplied NH_3 /NOx ratios of α 1.5, excess ammonia, α 1.0, balanced ammonia, and α 0.5, deficient ammonia. Levels of NO, NO_2 and NH_3 have been measured both upstream and downstream of the SCR using a gas analyser fitted with ammonia scrubbers to give reliable NOx measurements. A CFD model based on the porous medium approach has incorporated a kinetic scheme available in the open literature. Comparison of CFD simulations with observed data is presented and the results are discussed. NOx conversion is significant in the first 30 mm of the brick for α 0.5 and in the first 90 mm for α 1.0 and 1.5. The ammonia level influences NOx conversion, which is generally under-predicted by the current model for α 0.5 and over-predicted for α 1.5. Measurements show that NO_2 conversion exceeds NO conversion in the first section of the monolith, which the model fails to predict.

INTRODUCTION

Selective catalytic reduction, SCR, with aqueous urea has become one of the primary methods of NOx reduction for both heavy and light-duty diesel applications over the past few years. The urea is thermally hydrolysed in the vehicle's exhaust to produce ammonia, which in turn reacts with the NOx over a catalyst. SCR technology is advantageous for light-duty applications as it has a minimal impact on fuel consumption and costs, yet has high NOx reduction efficiencies [1], and [2].

NOx reduction is affected by the exhaust gas temperature. For low gas temperatures the fast SCR reaction is the dominant reaction where approximately equi-molar quantities of NO and NO_2 are present in the exhaust. The amount of NH_3 injected requires careful control, and can be critical under some conditions. Over-injection of NH_3 into the exhaust could potentially provide a high NOx conversion, but is likely to result in NH_3 slip [3]. The addition of an NH_3 oxidation catalyst downstream of the SCR is an option, but this may cause NO formation, which in turn will result in the vehicle not complying with emissions standards [4]. Under-injection of NH_3 will avoid NH_3 slip, but will provide an inferior NOx conversion.

The control of the NO_2: NOx ratio in the exhaust stream and the amount of NH_3 injected into the exhaust at any one time are therefore very important. This can be investigated experimentally, but this is a time consuming process and is not cost effective [5]. Simulation modelling can be considered a useful tool in reducing development time and costs.

Many models predict and compare conversion rates at the exit from the SCR, but neglect what is happening within the monolithic catalyst brick. This paper investigates the spatial conversion profile along the length of the SCR brick to provide a more thorough examination of the model using the porous medium approach in CFD. This approach has already been applied successfully to other catalysts [6] as well as SCRs [7], [8]. Ammonia gas, 5% in nitrogen, was substituted for urea spray in the experiments that are described in this paper to provide good control of the amount of ammonia injected. This also simplified the modelling, as there was no requirement to model either droplet evaporation or urea hydrolysis, thus focusing this investigation on the SCR CFD model itself.

ENGINE TEST RIG

The engine used in these experiments is a 1998cc 4-cylinder light-duty diesel engine with a common rail fuel injection system, an intercooled turbocharger, and EGR, which was de-activated to promote adequate levels of NOx solely for the purpose of model validation. The engine is connected to a 150 AC engine dynamometer. The test exhaust system consists of an interchangeable DOC/DPF assembly with an instrumentation module downstream and an SCR assembly with an instrumentation module both up and downstream. Before the gas enters the SCR it travels through a long narrow-angled 10 ° diffuser so that a uniform flow profile is presented to the inlet of the SCR brick. An expansion box followed by a converging nozzle was positioned just after the DOC/DPF assembly to ensure uniform flow before entering the diffuser. This means that a 1D model can be used for the simulations. A schematic of the engine/exhaust configuration is displayed in Figure 1.

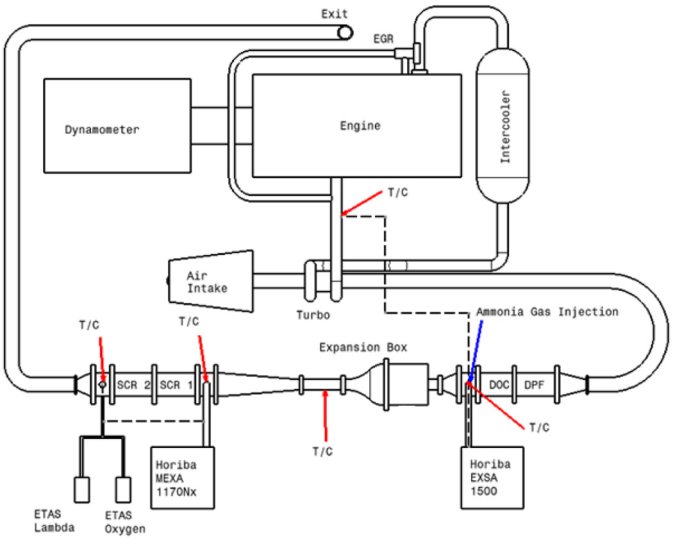

Figure 1. Experimental exhaust test rig. T/C indicates location of a thermocouple.

The 5% NH_3 gas in balance-N_2 was delivered into the exhaust at the instrumentation module downstream of the DOC/DPF assembly. The gas feed was controlled by manual valve and monitored by a flow meter with both glass and steel floats. Three different injection ratios were chosen based on the NOx level emitted by the engine, namely NH_3: NOx ratio α having values 0.5, 1.0 and 1.5.

The SCR catalysts were made of a base-metal zeolite, which had been de-greened for a period of 24 hours in a hydrothermal oven prior to testing at a temperature of 650 °C. The catalysts were 115 mm in diameter and ranged from 0.3 to 2.0 litres. Table 1 displays a full list of the dimensions and space velocities of the SCRs investigated.

Table 1. Dimensions of SCR bricks tested

Length (mm)	Capacity (litres)	GHSV (h^{-1})
30.5	0.3	531500
45.5	0.5	318000
60.7	0.6	265300
76.0	0.8	198800
91.0	1.0	159800
121.5	1.3	122100
136.5	1.5	106100
167.0	1.8	89000
182.0	2.0	80300

The oxidation catalyst was placed in an assembly with the DPF upstream of the SCR, and could be positioned before or after the DPF. Two DOCs were available for testing with volumes of 1 and 2 litres, providing space velocities of 1598000 and 80300 h^{-1} respectively. It is widely acknowledged that the optimum NO_2: NOx concentration ratio is 0.5. This ratio has been found to provide the optimum NOx reduction via the fast SCR reaction, which is active at low temperatures [5], [9], and [10]. The configuration that provided a value closest to this was a 1 litre DOC, corresponding to a GHSV of 159800 h^{-1}, placed downstream of the DPF.

Emissions were measured using a Horiba EXSA gas analyser at the engine outlet; this monitored the total NOx, CO/CO_2, and HC emissions from the engine using CLD, NDIR, and FID respectively. A Horiba MEXA-1170 analyser was used to measure NOx and NH_3 before and after the SCR brick via CLD. Previous work in this area had shown that the presence of NH_3 could influence the measured NOx value because the ammonia reacted with NO_2 on the internal NOx converter catalyst [8], [11], leading to erroneous measurements. Based on these issues and recommendations, ammonia scrubbers were fitted in to the MEXA analyser. The scrubbers are

designed to eliminate the ammonia before the sample gas enters the NOx converter within the analyser.

An engine condition of 1500rpm with 6 bar brake mean effective pressure (BMEP) was chosen for the experiments and this was comparable with previous studies, [8]. Exhaust gas temperatures were measured using K-type thermocouples at designated points along the exhaust as shown in Figure 1. Temperatures were 280 °C at the engine outlet, 260°C at the DOC/DPF assembly, and 215°C upstream of the SCR.

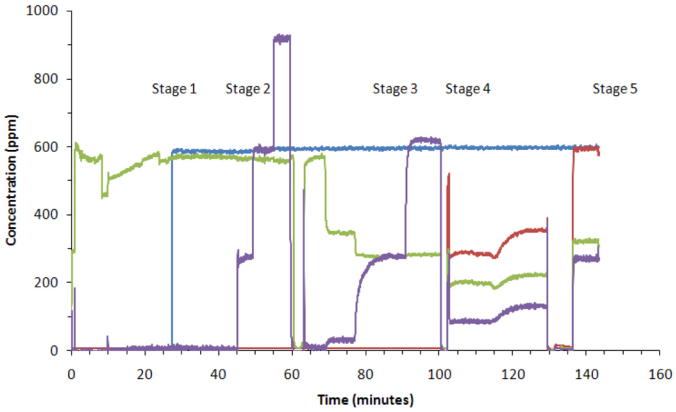

Figure 2. Example of plot of experimental logged data to illustrate test procedure. Stages 1-5: Blue, NOx; from engine Stages 1-2: Green, NOx; upstream of SCR Stage 2: Purple, NH_3; upstream of SCR Stage 3: Green, NOx; Purple NH_3; both downstream of SCR Stage 4: Red, NOx; Green, NO_2; Purple NO; all downstream of SCR Stage 5: Red, NOx; Green, NO_2; Purple NO; all upstream of SCR

Figure 2 displays an example of the output that was obtained by using a rigorous test procedure that was applied to each brick length. For the first 10 minutes of each test, the engine ran at 1500 rpm and 4 bar BMEP to allow the water and oil to reach operating temperature. The engine was then run at 1500 rpm and 6 bar BMEP for 35 minutes to allow steady state temperatures along the exhaust to be achieved. Table 2 displays the measurement modes and locations of the MEXA gas analyser sampling probe, and the NH_3: NOx injection ratios denoted by α. During these tests, NO_2: NOx ratio was close to 0.5.

Table 2. Five stages of experimental procedure, as illustrated in Figure 2.

Stage No.	MEXA analyser location	Measurement	α
1	Upstream of SCR	NOx	-
2	Upstream of SCR	NH_3 , NOx	0.5, 1.0, 1.5
3	Downstream of SCR	NH_3 , NOx	0.5, 1.0, 1.5
4	Downstream of SCR	NO , NO_2, NOx	1.5, 1.0, 0.5
5	Downstream of SCR	NO, NO_2, NOx	-

In Figure 2, the stage 1 measurement establishes the NOx level upstream of the SCR, and in stage 2 the three ammonia input levels that provide the three α values are measured, with α increasing during the stage. It is noticeable that the MEXA NOx measurement falls slightly relative to the EXSA NOx measurement between 55 and 60 minutes when excess ammonia is present even though the MEXA is fitted with scrubbers. In stage 3 the transient output of NOx and ammonia from the SCR is measured in response to the three different α conditions, with α increasing through the stage. Stage 4 measures the SCR outlet values of NO and NO_2 for the same three levels of ammonia input, but with α decreasing through the stage. Stage 5 measures the NOx input level for comparison with the earlier measurements in Stages 1 and 2. Also measured at stage 5 are the NO and NO_2 components. The measurements at stage 5 are made in the absence of ammonia. At stages 3 and 4, where measurements are made downstream of the SCR, steady state values can be deduced where the traces level off.

CFD MODEL

The CFD package used was Star-CD Version 4.10 and the monolithic catalysts were modelled using the porous medium approach [8]. The mesh used to represent the monolith was a simple rectangular block of 5 cells × 5 cells × 91 cells, with dimensions 10mm × 10mm × 364mm. Simulations with smaller cell sizes showed that this number of cells was sufficient to provide a mesh independent solution. The SCR kinetics used for the CFD model can be found in the literature, [12], where all the reaction rate constants are specified in full. The scheme contains the following SCR reactions [12]:

Standard SCR:

$$4NH_3 + 4NO + O_2 \rightarrow 4N_2 + 6H_2O \quad (1)$$

Fast SCR:

$$2NH_3 + NO + NO_2 \rightarrow 2N_2 + 3H_2O \quad (2)$$

Slow SCR:

$$4NH_3 + 3NO_2 \rightarrow 3.5N_2 + 6H_2O \quad (3)$$

N_2O Formation:

$$2NH_3 + 2NO_2 \rightarrow N_2 + N_2O + 3H_2O \quad (4)$$

Ammonia oxidation and reversible NO oxidation reactions are also included in the scheme, and are specified by reactions (5) and (6) respectively:

$$2NH_3 + 1.5O_2 \rightarrow N_2 + 3H_2O \quad (5)$$

$$NO + 0.5O_2 \leftrightarrow NO_2 \quad (6)$$

Equations (7) and (8) are the transport equations for the scalar species that represent the reactants. Reactions are assumed to take place in the pore phase of the model. The source terms in equations (7) and (8) were input into user subroutines for mass transfer in the CFD model for the pore and gas phases respectively [8].

$$\varepsilon \frac{\partial}{\partial t}[\rho_{Air} C_{iSol}] = \{K_{i\,m} \rho_{Air} A_V [C_{i\,Gas} - C_{i\,Sol}] + MR_{i\,Tot}\}[\frac{\varepsilon}{V_w}] \quad (7)$$

$$\varepsilon \frac{\partial}{\partial t}[\rho_{Air} C_{iGas}] + \frac{\partial}{\partial z}[\rho_{Air} U_S C_{i\,Gas}] = -K_{i\,m} \rho_{Air} A_V [C_{i\,Gas} - C_{i\,Sol}] \quad (8)$$

The reaction rate in (7) is multiplied by the stoichiometric coefficient for each reaction. The surface coverage relationship for ammonia sites stated by Olsson et al. [12] is given by equation (9).

$$\frac{\partial \theta}{\partial t} = \sum[\text{Stoichiometric coefficent} \times \text{Rate}] \text{ mol/mol-site/s} \quad (9)$$

This is interpreted within the Star-CD CFD model as:

$$\varepsilon \rho_{Air} \frac{\partial \theta}{\partial t} = \frac{\varepsilon \rho_{Air}}{\Omega} [R_{ads} - R_{des} - R_{Consumption}] \quad (10)$$

where all rates are in mol/m^3 monolith/s and the ammonia capacity of the substrate has value Ω mol-sites/m^3 monolith. Olsson et al. [12] use a value of 200 mol-sites/m^3 substrate. A nominal value of 400 mol-sites/m^3 is used here. In the CFD model, however, the number of available active sites is determined by the temperature of the solid phase, with factor $(293/T)^2$ applied to allow for local temperature. This gives an approximate value of 140 mol-sites/m^3. The model uses the multiplier of desorption rate activation energy as (1 - 0.98θ), as specified by Olsson et al [12], although this is notably different from the value (1-0.31θ) used in [13] and (1-0.545θ) used in [14].

The energy equations are solved for the fluid and solid phases of the analogous porous medium that represents the SCR monolith. Heat transfer between gas and solid phases is modelled through specification of heat transfer coefficients. The heat conduction within the solid phase of the monolith is calculated by specifying an effective bulk thermal conductivity.

Pressure loss along the porous medium is calculated within Star-CD via equation (11) by adjusting the permeability coefficients α and β.

$$\frac{\Delta P}{L} = -\alpha U_S^2 - \beta U_S \quad (11)$$

The inlet conditions for the steady state CFD simulations are given in Table 3. These were obtained from the measurements at the entrance to the SCR on the engine test bed. The NO and NO_2 values were representative of the engine test bed experiments for the eight different brick lengths. The output from the CFD simulation for all the SCR brick lengths investigated, Table 1, was obtained from a single run for each α value.

Table 3. Parameters for steady state CFD simulations

Parameter	Simulation 1	Simulation 2	Simulation 3
Mass flow rate (g/s)	31.0	31.0	31.0
Temperature at SCR inlet (K)	486	486	486
SCR brick length (mm)	182	182	182
NO inlet (ppm)	308	308	308
NO_2 inlet (ppm)	268	268	268
O_2 inlet (%)	11.38	11.38	11.38
NH_3 inlet	292	583	875
NH_3:NOx ratio, α	0.5	1.0	1.5
NO_2:NOx ratio	0.47	0.47	0.47
SCR capacity (mol-sites/m^3) at 293 K	400	400	400

MEASUREMENTS FROM TEST EXHAUST COMPARED WITH STEADY-STATE SIMULATIONS

The engine tests provided measurements of spatial species conversion along the SCR for α values 0.5, 1.0, and 1.5 under steady state conditions. The output from the CFD simulations was plotted for comparison with the measured data. Figure 3 plots the steady state spatial conversion rates for NOx and NH_3 for α 0.5, 1.0, and 1.5. When a deficient amount of NH_3 is injected, α 0.5, NOx reduction approaches 50% by about 90mm from the inlet; at this point all of the ammonia is consumed and NOx slip occurs. It can be seen that the NOx conversion just after the inlet to the SCR is under-predicted for α 0.5, but predictions agree much more closely with the data for brick lengths greater than 90 mm. For α 1.0, the agreement between the simulation and the experiment is significantly better all along the SCR brick. The balanced NOx and NH_3 conversion rates are to be expected for α 1.0 as approximately stoichiometric quantities of ammonia are available to convert the NOx. Conversion of NOx is slightly over-predicted by the model for all brick lengths for α 1.0. When excess ammonia is injected, α 1.5, the measured NOx

conversion is similar to the α 1.0 case. It can be seen that conversion is significantly over-predicted by the model in this case for the first 90 to 120 mm of the monolith. The difference between the simulation and the data is negligible by 182 mm.

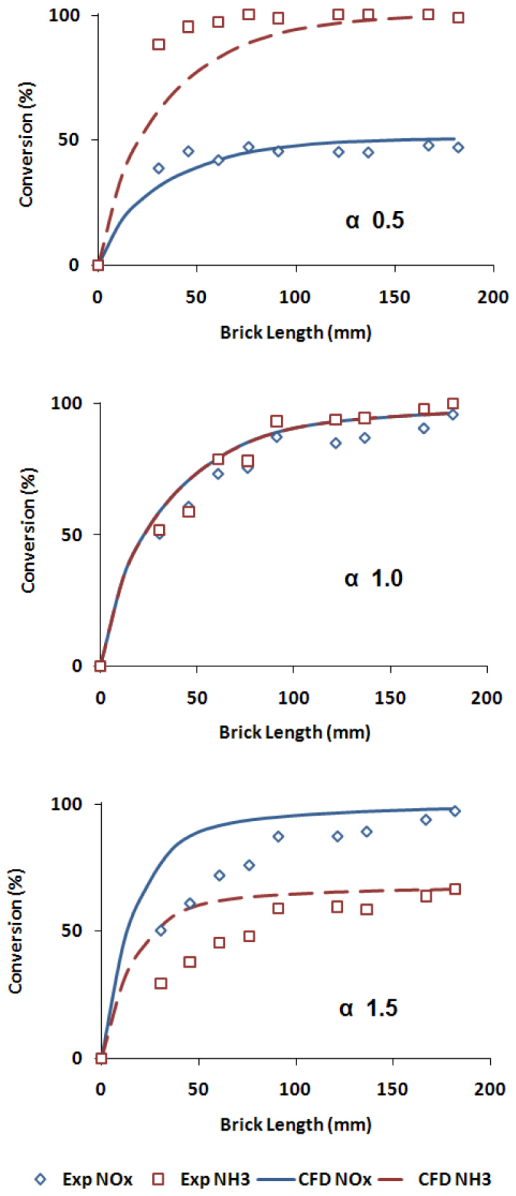

Figure 3. Spatial NOx and NH_3 conversion profiles: engine test data, symbols; CFD simulations, lines.

Comparisons between experimental data and the model for NO, NO_2, and NH_3 are presented in Figure 4 as conversion efficiency profiles. Figure 5 shows the same information as Figure 4 but plotted directly as species concentration profiles for the three values of α. For α 0.5 the correlation between the model and the experiment is relatively poor for NO_2 and NH_3 along the first half of the brick, although better for NO. The test data show that just after the SCR inlet the amount of NO_2 consumed is double that of NO. Agreement between both NO_2 and NH_3 data and the model is better towards the end of the brick, but is less good for NO around 150 mm brick length. When α is 1.0 an improved agreement between the test data and predictions is seen when compared with α 0.5. The model over-predicts the NO conversion throughout but NH_3 and NO_2 conversion are well predicted. The measured conversion rate for ammonia for α 1.5 is lower than for the other two injection conditions because ammonia is in excess. The measured conversion rates for NO are similar at α 1.0 and α 1.5; the same is true for NO_2. For α 1.5 the conversion of NO_2 approaches 100% at 90 mm whereas the conversion of NO approaches 100 % at 180 mm. The simulation agrees more closely with the data for NO_2 than for NO in this case.

To summarise the observations, the correlation between data and simulations is particularly poor in the first half of the SCR monolith for α 0.5 and α 1.5. Correlation between data and simulation is generally better for longer SCR brick lengths and is good in all cases at the brick exit. The CFD model under-predicts conversion rates for α 0.5 and over-predicts conversion rates for α 1.5. The model generally fails to predict the more rapid depletion of NO_2 compared with NO as the reactants enter the monolith.

MEASUREMENTS FROM TEST EXHAUST COMPARED WITH TRANSIENT SIMULATIONS

For two of the brick lengths investigated in the steady state tests, transient simulations have been performed using the 1D SCR CFD model. The parameters for the transient simulations are given in Table 4. The two brick lengths investigated were 31 mm and 91 mm. The data was taken from Stage 3, see Figure 2, for each experiment.

Table 4. Parameters for transient CFD simulations

Parameter	Simulation 1	Simulation 2
Mass flow rate (g/s)	31.0	31.0
Temperature at SCR inlet (K)	486	486
SCR brick length (mm)	31 (1/3 SCR brick)	91 (1 SCR brick)
NO inlet (ppm)	324	315
NO_2 inlet (ppm)	271	288
O_2 inlet %	12.2	12.0
NH_3 inlet stage 1	0 (0 – 237 s)	0 (0 – 99 s)
NH_3 inlet stage 2 (α 0.5)	292 (237 – 727 s)	292 (99 – 531 s)
NH_3 inlet stage 3 (α 1.0)	589 (727 – 1562 s)	590 (531 – 1865 s)
NH_3 inlet stage 4 (α 1.5)	879 (1562 – 2000 s)	880(1865 – 2650 s)
SCR capacity (mol sites /m^3 substrate) at 293 K	400	400

Figure 6 displays a comparison between data and simulation for case 1, with a short SCR brick 31 mm in length. In this simulation, the ammonia level input at 237 s is about half of the estimated requirement for conversion. The amount input at 727 s approximates to the amount required to fully convert the NOx. The amount input at 1562 s is about one and a half

times the estimated requirement, with consequential ammonia slip. Only the phase between 727 and 1562 s is simulated approximately correctly once steady state conditions are achieved. Between 237 and 737 s, NOx conversion is under-predicted. After 1562 s NOx conversion is over-predicted. This endorses the steady state results. The transient slip of ammonia after 727 s is not well predicted with the characteristic time for the data curve being much greater than for the simulation.

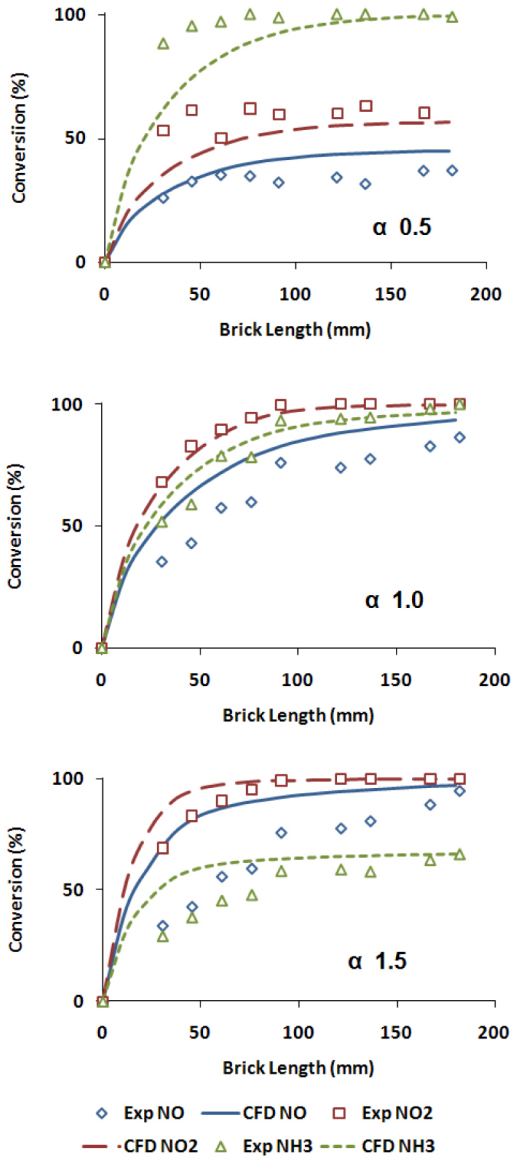

Figure 4. Spatial species conversion profiles: experimental data, symbols; simulations, lines.

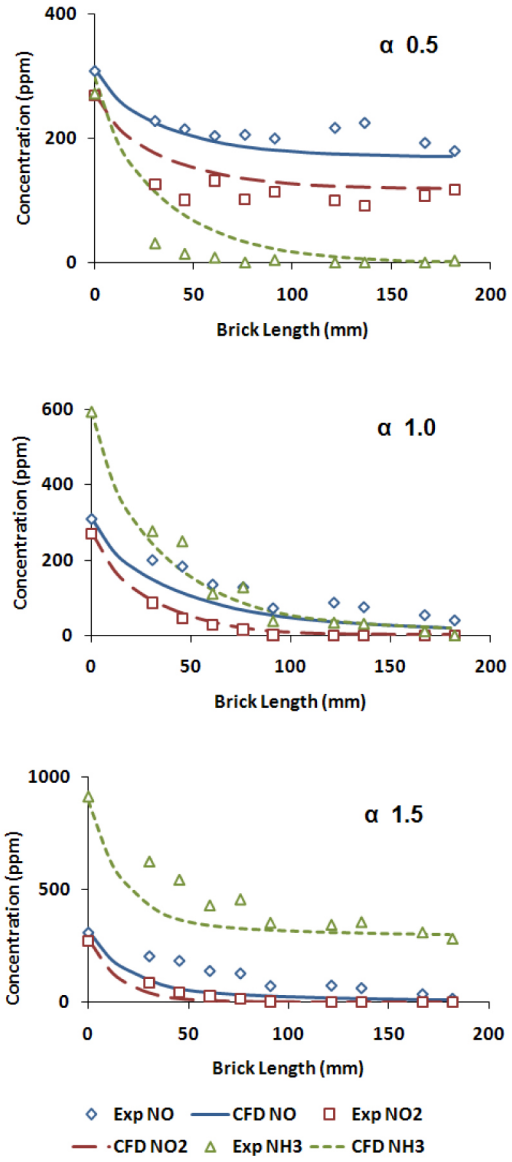

Figure 5. Spatial species concentration profiles: engine data, symbols; simulations, lines.

Figure 7 shows a corresponding comparison for case 2, with an SCR brick 91 mm in length. In this simulation, the ammonia level input at 99 s is about half of the estimated requirement for conversion. The amount input at 531 s approximates to the amount required to fully convert the NOx. The amount input at 1865 s is about one and a half times the estimated requirement, with consequential ammonia slip. All three phases are simulated approximately correctly, which endorses the steady state results for longer brick lengths. Ammonia slip between 727 and 1562 s is over-predicted; there is a delay in the experiment between 531 and about 900 s before ammonia slip is detected. The significant NOx slip after 2000s is also not predicted.

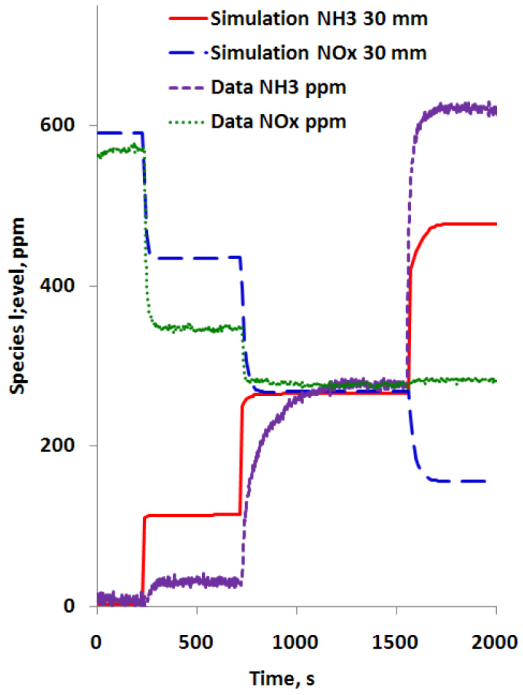

Figure 6. Comparison of simulation with transient data for case 1, 31 mm SCR brick

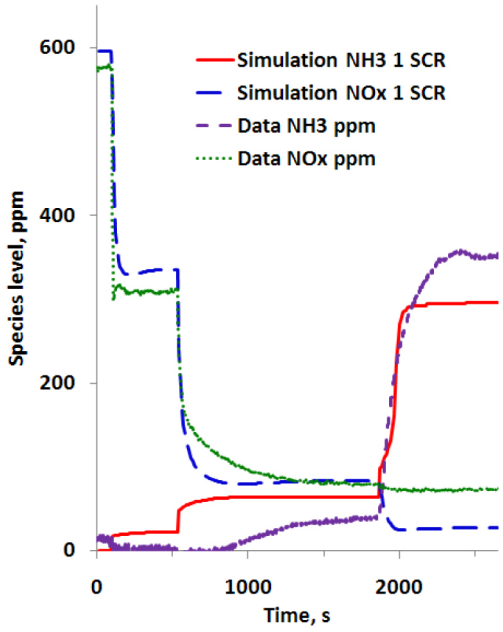

Figure 7. Comparison of simulation with transient data for case 2, 91 mm SCR brick

DISCUSSION OF RESULTS

In this study, the amounts of NH_3 consumed in every case are approximately equal to the NOx consumed. This suggests that reactions that compete with SCR, such as NH_3 oxidation, have a negligible effect on SCR NOx conversion under the steady state and low temperature conditions investigated.

The majority of NOx conversion that took place in the experimental exhaust occurred in the first 30mm of the SCR for α 0.5, and the first 90mm for α 1.0 and 1.5. Comparing the data for all three values of α with the simulations suggests that NOx conversion is under-predicted for deficient ammonia and over-predicted for excess ammonia for short bricks. The model is a reasonable description of the NOx data only when α is 1.0. This could suggest that the number of available reaction sites in the short bricks becomes less as α increases, or that the reactions are chemically inhibited in some other way when ammonia is present in excess. Grossale et al. [15] have proposed a mechanism for blocking of the fast SCR reaction at low temperature. There is no ammonia inhibition term in the SCR reactions in the Olsson et al. [12] chemical scheme and the ammonia storage capacity is constant. The number of reaction sites available in the experimental catalyst is apparently higher than in the model so that NOx conversion is under-predicted at short brick lengths for α 0.5. The observations indicate that the ammonia level influences the NOx reduction but that the current model does not adequately describe this effect. The CFD model was subjected to a parameter study, where the storage capacity of the bricks was varied from 200 to 500 mol-sites/m^3 before temperature correction. This supported the argument that as alpha increases conversion rates are inhibited, but simply changing the number of sites within a realistic range was insufficient to force the model describe all the data.

The simulation model predicts conversion efficiency reasonably well for NO_2 at α 1.0 but over-predicts NO_2 for short brick lengths at α 1.5 and under-predicts for α 0.5. The model also over-predicts conversion efficiency of NO at α 1.0 and severely over-predicts NO at α 1.5, but predicts quite well for α 0.5. For α 1.5, NO conversion continues beyond 90 or 100 mm even though all of the NO_2 has been consumed. This suggests that reaction (1) is effective under excess ammonia conditions despite the low temperatures in the exhaust. Although the results downstream of the full length SCR present a very strong correlation between the test data and the model, it is clear from this study that the model requires adjustment to improve data predictions just downstream of the inlet of the SCR and for short brick lengths.

The higher NO_2 conversion with respect to NO that is observed in the engine tests suggests significant low-temperature activity of reactions between NO_2 and NH_3. The kinetic scheme that has been used, however, includes slow SCR and N_2O formation but does not include side reactions between NO_2 and NH_3 such as nitrate formation, which can occur at low temperature. In this study NO_2:NOx ratios are ≤ 0.5 so nitrate formation is less likely to occur. It is observed

for the test data that just after the SCR inlet, after about 30 mm, the amount of NO_2 consumed is double that of NO, which is consistent with reaction (2) and reactions (3) and (4) occurring together. It is also noted that less NO is being converted in the experiment than in the model for α 1.0 and 1.5; this suggests that reaction (2) has too high a rate in the model. In the experiments reactions (3) and (4) may be influential on NOx reduction as by about 90mm NO_2 is the first species to be completely consumed for α 1.0 and 1.5, and this cannot be explained by the fast SCR reaction alone. Once all of the NO_2 has been consumed in the experiments, the reduction of NO continues slowly, because reaction (1) has a fairly low rate at the temperature of the experiment. In the model, the fast reaction has the highest rate just downstream of the SCR brick inlet with reactions (1), (3) and (4) an order of magnitude slower. Overall for the steady state cases, the simulated data provides a good representation of experimental data downstream of the longest SCR, but agreement in the first 90mm is poor. The transient simulations provide only moderate agreement with the engine data for 31 and 91 mm SCR bricks. The adsorption and desorption of ammonia will be influential in the transient model and it may be necessary to change the dependence of the ammonia desorption activation energy on ammonia level in order to improve agreement between the model and the transient observations of ammonia and NOx slip.

CONCLUDING REMARKS

A comparison between the spatial conversion profiles of a mathematical model using the porous medium approach and engine test data using ammonia gas, as well as transient NH_3 adsorption/desorption is presented. The following observations were made:

• The majority of NOx conversion that took place in the experimental exhaust occurred in the first 30mm of the SCR for α 0.5, and the first 90mm for α 1.0 and 1.5.

• The higher NO_2 conversion with respect to NO observed in the engine tests suggests significant low-temperature activity of NO2 + NH_3 reactions. These comprise slow SCR and N_2O formation and could involve side reactions between NO_2 and NH_3, such as nitrate formation, not included in the kinetic scheme employed in this study.

• Under deficient ammonia conditions, the agreement between steady state experimental data and simulated data is poor just after the SCR inlet, and this is also noted for excess ammonia. This suggests that the ammonia level influences the NOx reduction but that the model does not adequately describe this effect. Agreement for stoichiometric ammonia conditions, however, was shown to be quite strong. The activity of NO_2 + NH_3 reactions was lower in the model than in the experiments with fast SCR being the dominant reaction in the model.

• The simulated data provides a good representation of experimental data downstream of the SCR, but agreement in the first 90mm is poor.

• The transient simulations provide only moderate agreement with the engine data for 31 and 91 mm SCR bricks, with better overall agreement for the 91 mm brick.

REFERENCES

1. Blakeman, P.G., Chandler, G.R., John, G.A., and Wilkins, A.J.J., "Investigations into NOx Aftertreatment with Urea SCR for Light-Duty Diesel Vehicles," SAE Technical Paper 2001-01-3624, 2001, doi:10.4271/2001-01-3624.

2. Tennison, P., Lambert, C., and Levin, M., "NOx Control Development with Urea SCR on a Diesel Passenger Car," SAE Technical Paper 2004-01-1291, 2004, doi: 10.4271/2004-01-1291.

3. Girard, J., Snow, R., Cavataio, G., and Lambert, C., "The Influence of Ammonia to NOx Ratio on SCR Performance," SAE Technical Paper 2007-01-1581, 2007, doi: 10.4271/2007-01-1581.

4. Gekas, I., Vressner, A., and Johansen, K., "NOx Reduction Potential of V-SCR Catalyst in SCR/DOC/DPF Configuration Targeting Euro VI Limits from High Engine NOx Levels," SAE Technical Paper 2009-01-0626, 2009, doi: 10.4271/2009-01-0626.

5. Chatterjee, D., Burkhardt, T., Rappe, T., Güthenke, A. et al., "Numerical Simulation of DOC+DPF+SCR Systems: DOC Influence on SCR Performance," *SAE Int. J. Fuels Lubr.* **1**(1):440-451, 2008, doi:10.4271/2008-01-0867.

6. Benjamin, S.F., Roberts, C.A.. "Three-dimensional modelling of NOx and particulate traps using CFD: A porous medium approach" Applied Mathematical Modelling 31 (2007) 2446-2460.

7. Benjamin, S.F., Roberts, C.A.. "The Porous Medium Approach to CFD Modelling of SCR with Injection of Urea-Droplets" (2007) Pro IMechE Conference (C66/047) 143-159.

8. Tamaldin, N., Roberts, C.A., and Benjamin, S.F., "Experimental Study of SCR in a Light-Duty Diesel Exhaust to Provide Data for Validation of a CFD Model Using the Porous Medium Approach," SAE Technical Paper 2010-01-1177, 2010, doi:10.4271/2010-01-1177.

9. Ciardelli, C., Nova, I., Tronconi, E., Chatterjee, D., Bandl-Konrad, B., Weibel, M., Krutzsch, B.. "Reactivity of NO/NO2-NH3 SCR system for diesel exhaust after-treatment: Identification of the reaction network as a function of temperature and NO2 feed content" Applied Catalysis B: Environmental 70 (2007) 80-90.

10. Nakayama, R., Watanabe, T., Takada, K., Odaka, M. et al., "Control Strategy for Urea-SCR System in Single Step

Load Transition," SAE Technical Paper 2006-01-3308, 2006, doi:10.4271/2006-01-3308.

11. Shah, S.D., Mauti, A., Richert, J.F.O., Loos, M.J. et al., "Measuring NOx in the Presence of Ammonia," SAE Technical Paper 2007-01-0331, 2007, doi: 10.4271/2007-01-0331.

12. Olsson, L., Sjovnall, H., Blint, R.. "A kinetic model for ammonia selective catalytic reduction over Cu-ZSM-5" Applied Catalysis B: Environmental 81 (2008) 203-217.

13. Chi, J.N. and DaCosta, H.F.M., "Modeling and Control of a Urea-SCR Aftertreatment System," SAE Technical Paper 2005-01-0966, 2005, doi: 10.4271/2005-01-0966.

14. Chatterjee, D., Burkhardt, T., Weibel, M., Nova, I. et al., "Numerical Simulation of Zeolite- and V-Based SCR Catalytic Converters," SAE Technical Paper 2007-01-1136, 2007, doi: 10.4271/2007-01-1136.

15. Grossale, A., Nova, I., Tronconi, E.. "Ammonia blocking of the fast SCR reactivity over a commercial Fezeolite catalyst for diesel exhaust aftertreatment". J. Catalysis 265 (2009) 141-147.

CONTACT INFORMATION

S. F. Benjamin
s.benjamin@coventry.ac.uk

ACKNOWLEDGMENTS

The authors would like to express their appreciation to Faurecia, Jaguar-Land Rover, and Johnson Matthey plc for their support. Robert Gartside of Coventry University provided valuable technical assistance. Funding by EPSRC UK is also gratefully acknowledged.

DEFINITIONS/ABBREVIATIONS

Symbols

A_V
: **Reactor surface area per unit volume (m^2/m^3)**

$C_{i\ Gas}$
: **Concentration of species i in the solid phase (mass fraction)**

$C_{i\ Sol}$
: **Concentration of species i in the solid phase (mass fraction)**

$K_{i\ m}$
: **Mass transfer coefficient of species i (m/s)**

L
: **Channel length (m)**

M
: **Molecular mass (kg/mol) for species i**

P
: **Pressure (N/m^2)**

R_i
: **Reaction rate for species I (mol/mol-site/s)**

$R_{i\ Tot}$
: **Total reaction rate for each species**

t
: **Time (s)**

T
: **Temperature (K)**

U_S
: **Superficial velocity (m/s)**

V_W
: **Pore volume per unit reactor volume (m^3/m^3)**

Greek Symbols

α
: **Permeability coefficient and NH_3: NOx ratio**

β
: **Permeability coefficient**

ε
: **Porosity of the substrate**

ρ
: **Density of air (kg/m^3)**

θ
: **Fraction of sites occupied by ammonia**

Ω
: **Number of reaction sites (mol-sites/m^3)**

Abbreviations

CFD
Computational fluid dynamics

CLD
Chemiluminescent detector

DOC
Diesel oxidation catalyst

DPF
Diesel particulate filter

FID
Flame ionisation detector

GHSV
Gas hourly space velocity (h^{-1})

NDIR
Non-dispersive infrared detector

SCR
Selective catalytic reduction

T/C
Thermocouple

The Engineering Meetings Board has approved this paper for publication. It has successfully completed SAE's peer review process under the supervision of the session organizer. This process requires a minimum of three (3) reviews by industry experts.

ISSN 0148-7191

doi:10.4271/2010-01-2089

SAE Customer Service:
Tel: 877-606-7323 (inside USA and Canada)
Tel: 724-776-4970 (outside USA)
Fax: 724-776-0790
Email: CustomerService@sae.org
SAE Web Address: http://www.sae.org
Printed in USA